^{4}He(^{4}He,^{3}He)^{5}He(g.s.) reaction at 118 MeV, and its distorted wave Born approximation interpretation

R. E. Warner,* J. M. Fetter,† and R. A. Swartz‡
Oberlin College, Oberlin, Ohio 44074

A. Okihana, T. Konishi, and T. Yoshimura
Kyoto University of Education, Kyoto 612, Japan

P. D. Kunz
University of Colorado, Boulder, Colorado 80309

M. Fujiwara
Research Center for Nuclear Physics, Osaka University, Osaka 567, Japan

K. Fukunaga,§ S. Kakigi, and T. Hayashi
Institute for Chemical Research, Kyoto University, Kyoto 606, Japan

J. Kasagi
Laboratory of Nuclear Science, Tohoku University, Sendai 982, Japan

N. Koori
University of Tokushima, Tokushima 770, Japan
(Received 22 September 1993)

The ^{4}He(^{4}He,^{3}He)^{5}He(g.s.) reaction was observed at 118 MeV for c.m. angles from about 30° to 120°. Distorted wave Born approximation (DWBA) calculations accurately predict the shapes of the ^{3}He spectra for $\epsilon_{\alpha n} \leq 2.5$ MeV, where $\epsilon_{\alpha n}$ is the relative energy of the final α-n system. However the measured differential cross sections are smaller than the DWBA predictions by about a factor of 2 at forward angles, and have a less pronounced minimum at 90° c.m. than the theory predicts.

PACS number(s): 25.55.Hp, 24.10.Eq, 27.10.+h

I. INTRODUCTION

Although single-nucleon transfer to final states with two bound nuclei is a mature field of study [1], transfer reactions to unbound states present greater challenges for both measurements and their theoretical interpretation. Measurements [2] may require detection of both fragments from the unbound decay, with attendant uncertainty in the coincidence detection efficiency.

We present here measurements of the ^{4}He(^{4}He,^{3}He)^{5}He(g.s.) reaction at 118 MeV, which are interesting for several reasons. First, since the two initial nuclei are identical, complete information is obtained by measurements to 90° c.m. Second, the distorted wave Born approximation (DWBA) approach is considered valid only when the bombarding energy is high compared with the binding energy of the transferred nucleon [3]; thus our energy may be high enough to suitably test the theory even though the transferred neutron is bound by 20 MeV in ^{4}He. Next, by detecting the final ^{3}He we achieve 100% detection efficiency, thereby observing final states including all directions of the α-n relative momentum vector in the ^{5}He system. Thus, the cross section in an incoherent sum of the partial cross sections over all (l, j) states of the α-n system [4]. In our experiment we lose any knowledge of the α-n correlations. This loss of knowledge overcomes difficulties of similar experiments [2], which have employed coincident α-n detection, with resulting directional bias in selection of ^{5}He decays and unknown efficiency [2,5].

Finally, predictions of the cross sections require distorted wave calculations, in which the numerical integrations converge slowly due to the presence of the unbound-state wave function. Ingenious computational techniques [4] have been devised to achieve sufficiently rapid convergence.

For example, we can perform the calculations in the post-stripping (^{4}He,^{3}He) representation using the technique of Vincent and Fortune [4] to obtain convergence. This calculation used the V_{n3} interaction (the subscript 3 denotes ^{3}He) but neglects the difference between the

*Present address: Physics Department, University of Michigan, Ann Arbor, MI 48109-1120.
†Present address: Physics Department, University of Wisconsin, Madison, WI 53706.
‡Present address: Physics Department, Indiana University, Bloomington, IN 47405.
§Present address: Yamagata University, Yamagata 990, Japan.

$V_{3\alpha}$ interaction and the α-α optical potential $U_{\alpha\alpha}$. Such neglect is usual and justifiable for reactions on heavier nuclei but questionable for such light nuclei. To evaluate the differences we have compared our calculations with the prior stripping which uses the interaction $V_{n\alpha}$ but neglects the difference between the $V_{3\alpha}$ interaction and the optical potential U_{3S}. Thus, we find agreement to about 10% between calculations. This agreement is remarkable considering the differences in the binding energies of the n-α and n-^{3}He systems, which are -0.89 and $+20.68$ MeV, respectively.

II. EXPERIMENTAL PROCEDURE

A 13-cm-diam gas cell containing ^{4}He was bombarded with 118.7-MeV α particles from the AVF cyclotron at the Research Center for Nuclear Physics (RCNP) of Osaka University. Energy losses in the entrance window (10-μm Havar) and in the gas (held at 3.05 ± 0.05 atmospheres absolute pressure) reduced the energy at target center to 118.0 MeV. The beam spot diameter was 2 mm, and beam currents were held between 2 and 8 nA to keep counting losses small.

Each of two ΔE-E Si telescopes concurrently detected ^{3}He particles from the ^{4}He(^{4}He,^{3}He)^{5}He reaction and α-particles from α-α elastic scattering. Each telescope had a transmission (ΔE) detector 100 μm thick and 100 mm^2 in active area, a stopping (E) detector 5 mm thick, and a lead front slit of 3 mm width placed 95 mm from the target center. The 3.5×6.5-mm rectangular rear slit of telescope A was 270 mm from target center; telescope B's 4.0×6.4 mm slit was 240 mm from the center.

Energy calibration was obtained from the angular dependences of both the maximum ^{3}He energies available from the ^{4}He(^{4}He,^{3}He)^{5}He reaction and the peaks in the ^{3}He spectra due to the ^{5}He ground state, for which $\epsilon_{\alpha n} = 0.89$ MeV and $\Gamma = 0.60$ MeV [6]. These data were consistent enough to determine the energy gain (MeV/channel) to an accuracy better than 2%.

Conventional electronics were used to gate a raw-data processor, through which signals were transmitted to a PDP 11/44 data acquisition computer. Scalers recorded both the total number of logic signals presented to the computer and the number accepted for processing; their ratio showed that dead times were less than 2%.

Particle identification (PID) and energy spectra were obtained off line; the PID spectra showed complete separation between the ^{4}He, ^{3}He, and $Z = 1$ groups.

III. EXPERIMENTAL RESULTS

First, 118-MeV α-α elastic differential cross sections were deduced from the yields of elastically scattered α particles. These were smaller than those previously reported [7] and were therefore renormalized. For this purpose interpolation was needed, since the previous measurements were made at slightly different energies. We found that 118-MeV cross sections could be obtained from the previously reported 99.60- and 119.86-MeV cross sections by three different procedures, whose results differed by less than 10%: interpolation between 119.86- and 99.6-MeV cross sections; calculations from phase shifts interpolated between those reported at those energies; or simple adoption of the 119.86-MeV cross section. The elastic angular distribution shown by the solid curve in Fig. 1 was obtained by interpolating phase shifts. The dashed curve shows an optical-model calculation described in Sec. IV.

Data from detectors A and B were renormalized by factors of 1.24 and 1.60, respectively. Since these factors differ, the counting losses must not have resulted from faulty measurement of charge or gas pressure; rather, we suspect inefficiency in triggering the data acquisition computer. The quality of fit in Fig. 1 indicates that the counting losses were time independent. Data from the two detectors agree to better than $\pm 10\%$ at angles where measurements were made with both, and we therefore believe our renormalization procedure to be reliable to this accuracy.

^{3}He energy spectra from the ^{4}He(^{4}He,^{3}He)^{5}He reaction were then obtained for comparison with DWBA predictions, which are later described in Sec. IV. Three typical fitted spectra are shown in Figs. 2–4; the solid curve shows the fit for $\epsilon \leq 5$ Mev, ϵ being the relative energy of the final α-n system. The fitting procedure included the effects of target thickness and finite detector geometry, and of energy resolution; the amplifier gain (which varied by about 2% from run to run) and the overall normalization were used as fitting parameters. Nearly all individual spectra were fitted with $0.8 \leq \chi^2/N \leq 1.2$ for $\epsilon \leq 2.5$ MeV. Thus, the DWBA accurately repro-

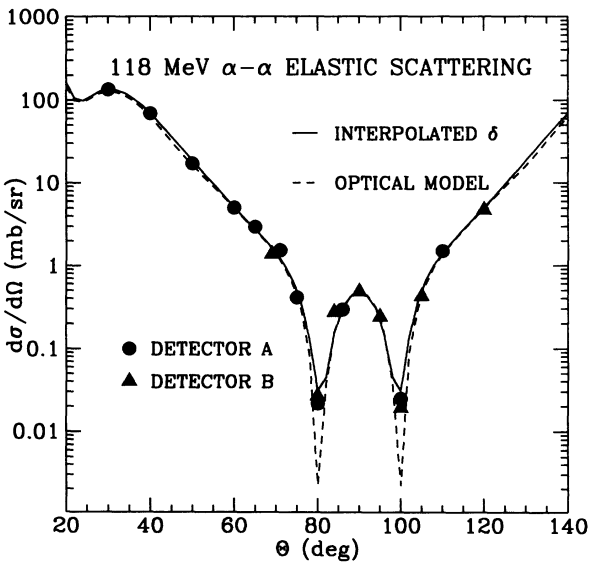

FIG. 1. α-α center-of-mass elastic scattering differential cross sections measured at 118 MeV, after renormalization as described in text. Data points for detector A are circles, those for detector B are triangles. Pairs of nearly identical data points (near 70° and 85° c.m.) measured with the two detectors are plotted with equal but opposite displacements from the true scattering angle, for clarity. Parameters for the optical-model calculation are given in Table II; phase shifts for the other calculation are interpolated from [7].

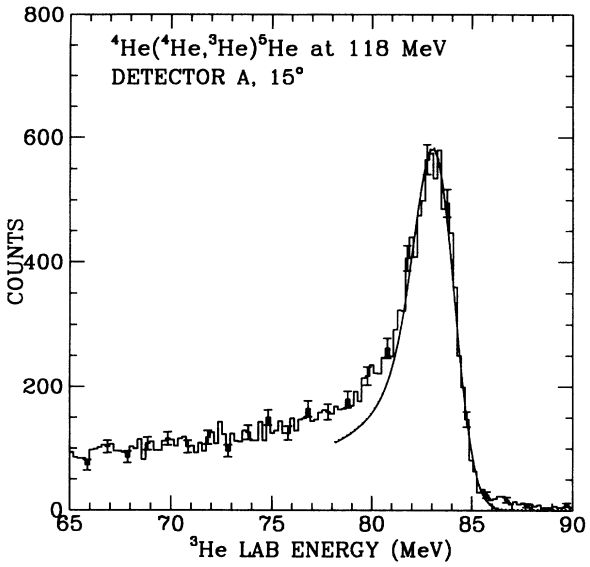

FIG. 2. Energy spectrum of ^{3}He from the ^{4}He(^{4}He,^{3}He)^{5}He reaction at 118 MeV at laboratory angle 15° (29.7° c.m.). The solid line shows the renormalized DWBA fit to the ^{5}He ground-state peak (for $0 \leq \epsilon_{\alpha n} \leq 5$ MeV; see text). Typical error bars are shown.

duces the shape of the ^{5}He(g.s.) peak (i.e., up to at least $\epsilon = 2.5$ MeV) but not, as we show next, its magnitude. We did not attempt to fit the spectra for $\epsilon \geq 5$ MeV since this region includes multistep, direct knockout, and other complicated processes not treated by the DWBA.

Magnitudes of the predictions and measurements are best compared through differential cross sections integrated over ϵ. From the data we deduce the yield Y of events between the highest ^{3}He laboratory energy permitted by three-body kinematics and some lower limit. To relate Y and the c.m. double-differential cross section

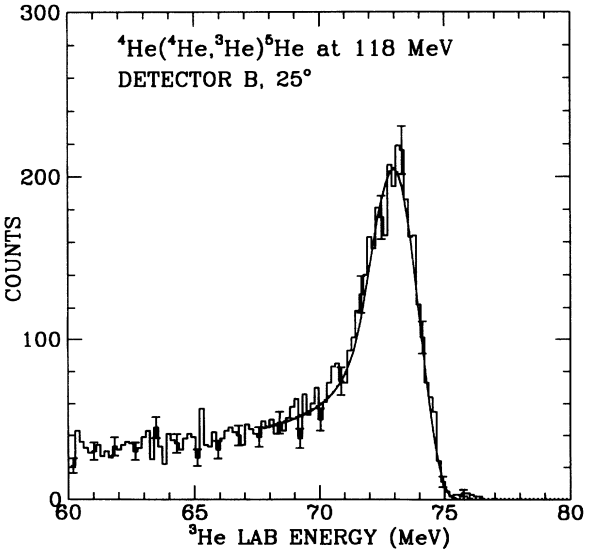

FIG. 3. Same as Fig. 2, for laboratory angle 25° (49.6° c.m.).

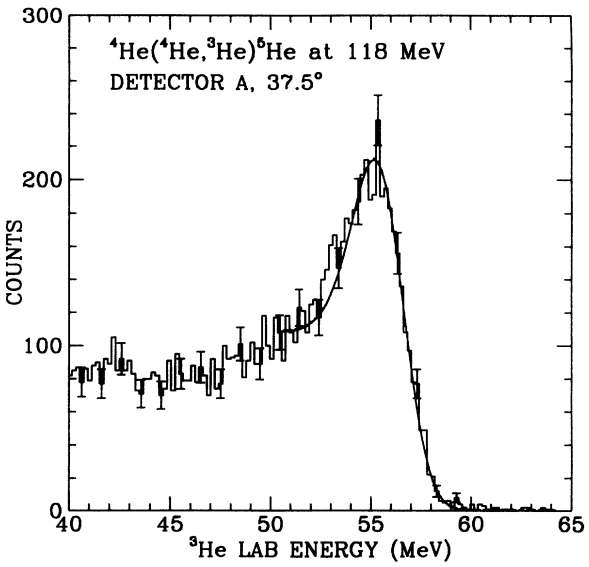

FIG. 4. Same as Fig. 2, for laboratory angle 37.5° (74.5° c.m.).

$\sigma(\epsilon,\theta)$ (expressed in mb/sr MeV) we generalize an earlier study [8] of elastic scattering from a gas target, and find

$$Y = nN \int dt \int d\Omega \int_0^{\epsilon^*} J[(\epsilon,\theta)\sigma(\epsilon,\theta)]d\epsilon \ , \qquad (1)$$

where there are n incident particles and N nuclei per unit volume in the target. Integration is over a detector laboratory solid angle Ω, the target thickness t visible from the detectors, and α-n relative energy ϵ. The c.m.-to-laboratory conversion factor J and the double-differential cross section vary with both ϵ and the c.m. scattering angle θ. The lower limit of the laboratory energy acceptance is chosen such that, for central rays, the upper integration limit ϵ^* of α-n relative energy is 5.0 MeV. (Thus, the counts included in the reported cross sections are those in channels for which a DWBA fit is shown in Figs. 2–4.) This value is arbitrary but convenient since (a) it fully includes the ground-state peak (see Figs. 2–4) and (b) it usually falls in a broad minimum of the spectrum. Typical ϵ^*'s for extreme rays are about 4 and 6 MeV at the laboratory cutoff energy.

We find the mean relative energy $\langle\epsilon\rangle$ by multiplying the integrand of Eq. (1) by ϵ and dividing the resulting integral by the original Y; in both calculations, $\sigma(\epsilon,\theta)$ has the ϵ dependence predicted by DWUCK. Similarly we find the mean c.m. scattering angle $\langle\theta\rangle$ and its mean-squared deviation $\langle\delta\theta_{\rm rms}\rangle$. We define a mean conversion factor $\langle J\rangle = J(\langle\epsilon\rangle,\langle\theta\rangle)$ and an integrated cross section

$$\sigma_{\epsilon^*}(\theta) = \int_0^{\epsilon^*} \sigma(\epsilon,\theta)d\epsilon \ . \qquad (2)$$

Upon finding that Y and

$$Y' = nN\langle J\rangle\sigma_{\epsilon^*}(\theta) \int\int dt\, d\Omega \qquad (3)$$

TABLE I. Measured differential cross sections for ^{4}He(^{4}He,^{3}He)^{5}He, integrated for $0 \leq \epsilon_{\alpha n} \leq 5$ MeV. The c.m. angles $\langle\theta\rangle$ and $\langle\delta\theta_{\rm rms}\rangle$ were determined as described in the text.

$\langle\theta\rangle \pm \langle\delta\theta_{\rm rms}\rangle$ (deg)	$d\sigma/d\Omega$ (mb /sr) Telescope A	Telescope B
29.7±0.9	5.35±0.05	
39.6±0.9	4.58±0.04	
49.6±1.0	3.21±0.03	3.09±0.05
59.5±1.1	1.49±0.02	1.42±0.03
64.4±1.0	1.05±0.01	
69.4±1.2	0.90±0.01	0.88±0.02
74.5±1.1	0.69±0.01	
79.5±1.3	0.50±0.01	0.48±0.01
84.5±1.3	0.29±0.01	0.32±0.01
89.6±1.4		0.22±0.01
94.4±1.5		0.30±0.01
99.3±1.6		0.48±0.01
104.1±1.7		0.69±0.01
118.5±1.9		1.26±0.02

generally agree within about 1% when $\epsilon^* = 5$ MeV for central rays, we concluded that measured differential cross sections are obtainable from the equation

$$\sigma_{\epsilon^*}(\theta) = Y/\left[nN\langle J\rangle \int\int dt\, d\Omega\right] . \quad (4)$$

The ^{3}He yields were renormalized by the same factors as the α-α elastic cross sections. Differential cross sections $\sigma_{\epsilon^*}(\theta)$, deduced from the renormalized yield, are presented in both Table I and Fig. 5. The normalization

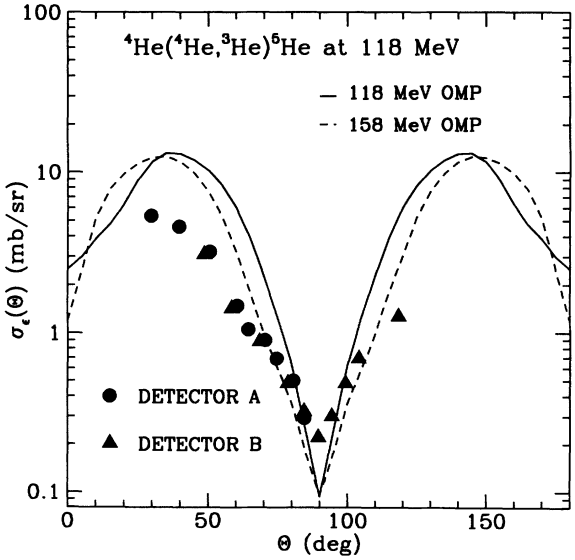

FIG. 5. Center-of-mass differential cross sections $\sigma_\epsilon(\theta)$ for the ^{4}He(^{4}He,^{3}He)^{5}He reaction, renormalized as described in text. Both data and predictions are integrated over the ^{3}He laboratory energy range in which $0 \leq \epsilon_{\alpha n} \leq 5$ MeV for central rays. As in Fig. 1, four pairs of nearly identical data points, measured with the two detectors, are horizontally displaced for clarity. DWBA predictions use the two α-α optical-model parameter sets of Table II.

is considered accurate to ±10%, and statistical uncertainties (from a minimum of 1200 events/run) are always smaller. Agreement of data from both telescopes, at angles where measurements were made with both, indicates the validity of the renormalization. This renormalization against the α-α elastic cross sections removes several possible errors: beam charge integration, gas pressure determination, solid-angle uncertainty, and dead time. It partially compensates for reaction-tail losses which, for α particles below 100 MeV [9], are less than 2%.

IV. DWBA CALCULATIONS AND COMPARISON WITH MEASUREMENTS

We used the program [10] DWUCK4, modified for an initial channel with two identical particles, to calculate the transition amplitude T_{fi}. This is described in the prior representation as

$$T_{fi} = \langle \chi_f^- \chi_{\alpha n}^- | V_{\alpha n} | \phi_{3n} \chi_i^+ \rangle . \quad (5)$$

The wave function ϕ_{3n}, for the bound n-^{3}He system in one of the initial α particles, was taken from Shepard, Rost, and Smith [11]; it fits the electron scattering data and includes hard-core effects. $\chi_{\alpha n}^-$ describes the α-n relative motion (with incoming-scattered-wave boundary conditions) in the final ^{5}He. The α-n interaction was taken to be a real Woods-Saxon well with spin-orbit coupling, which fits the energy dependence of the p-α phase shifts [5]; the real central well depth was changed from 45.96 to 46.71 MeV to correctly locate the ^{5}He ground-state peak.

The α-α relative wave function χ_i^+ in the incident channel was obtained for a conventional Woods-Saxon (WS) potential plus a second real WS potential with range less than 1 fm. This optical-model potential (OMP) was found by starting with a similar OMP (potential 2, Ref. [12]) used to fit 158-MeV α-α elastic scattering data, and changing the parameters to fit the existing 120-MeV data [7]. This potential (called, hereafter, the "118-MeV potential") is compared with the 158-MeV potential in Table II. The fit to our 118-MeV α-α elastic scattering data achieved with the 118-MeV potential is shown in Fig. 1 by a dashed line. The 118-MeV α-α potential was also used to find the distorted wave χ_f^- for the relative motion of the ^{3}He and ^{5}He centers of mass. c.m. double-differential cross sections for the $p_{3/2}$ and $p_{1/2}$ states of ^{5}He were calculated from the formula [5]

$$\sigma^{jl}(\epsilon,\theta) = \left(\frac{\mu k}{\pi\hbar^2}\right)\left(\frac{2j+1}{2l+1}\right) D_0^2 \sigma_{\rm DW}^{jl} . \quad (6)$$

μ is the reduced mass, k is the relative wave number, and ϵ is the relative energy for the α-n system. The $p_{1/2}$ cross section was typically only a few percent of that for the $p_{3/2}$ state, as is expected since the $p_{1/2}$ phase shifts are much smaller [13] and the factor $(2j+1)$ causes further reduction. Similarly, the $s_{1/2}$ contribution is expected to be still smaller.

Since the final state of this reaction is unbound, the

TABLE II. Optical-model parameters for the α-α interaction used at 158 MeV (Ref. [11]) and in the present work at 118 MeV. Energies are in MeV, distances in fm.

E_0	V	r_0	a_0	W_v	r_w	a_w	V'	r'_0	a'_0
118	48.55	1.792	0.596	8.580	2.202	0.287	64.50	0.632	0.243
158	53.75	1.628	0.613	9.623	2.094	0.467	43.97	0.545	0.142

calculations must be performed in zero range, with the code DWUCK4. All nonlocality parameters were set to zero. The strength D_0^2, which is known [14] to be about 20×10^4 MeV fm^{-3} for (^{4}He,^{3}He) on heavier targets and at lower energies, must be recalibrated for 59-MeV c.m. energy and a target as light as ^{4}He. We accomplish this by assuming the final ^{5}He state to be bound by 0.1 MeV, and then performing both zero-range and full finite-range calculations, the latter with the code DWUCK4. For this auxiliary calculation a realistic (^{4}He,^{3}He) form factor [14] was used which accounts for the normalization of this reaction in heavy targets over a wide range of energies. The ratio of the finite-range and zero-range differential cross sections gave $D_0^2 = 4.8 \times 10^4$ Mev fm^{-3} at 59-MeV c.m. When the same comparison was made for the ^{48}Ca(^{3}He,^{4}He)^{47}Ca reaction, $D_0^2 = 18 \times 10^4$ MeV fm^{-3} was obtained at both 23- and 60-MeV c.m. The large reduction in our case seems to be due to the extreme surface nature of ^{4}He.

The $p_{3/2}$ and $p_{1/2}$ cross sections were added incoherently to obtain the double-differential cross sections $\sigma(\epsilon, \theta)$ used to fit the energy spectra in Figs. 2–4.

DWBA predictions of σ_ϵ (θ), obtained with Eq. (2) for both α-α optical potentials listed in Table II, are also shown in Fig. 5. The two predictions are similar in that they both generally overpredict the measured data while reaching lower minima at 90° c.m. However, the potential specifically devised to fit the 118-MeV elastic scattering data peaks at a somewhat larger angle (near 40° c.m.) in contrast to the measurements and the 158-MeV prediction.

V. DISCUSSION AND CONCLUSIONS

The DWBA predictions accurately predict the shapes of most individual angle spectra near the ^{5}He ground-state peak, up to an α-n relative energy $\epsilon_{\alpha n}$ of about 5 MeV. However, some of the small-angle spectra (see Fig. 2) show discrepancies between measurement and predictions at excitation energies from about 3 to 5 MeV. These discrepancies amount, at most, to 10% of the area which was fitted. They may result, in part, from processes not treated by the DWBA such as direct three-body breakup.

The angular dependence of the integrated cross sections, shown in Fig. 5, is less well described by the DWBA. The predicted minimum at 90° c.m. is too deep, and the forward-angle cross sections are overpredicted by about a factor of 2. This overprediction would be still greater, though by a very small amount, if the DWBA gave sufficient strength to fit the forward-angle spectra in the region $\epsilon = 3$–5 MeV. There is little to choose between the two optical potentials employed, except that the 158-MeV potential gives results closer to the 60° to 80° measurements.

The overprediction of the integrated cross sections is significant, since we had to use a finite-range renormalization factor D_0^2 only one-fourth as large as that used for the (^{4}He,^{3}He) reaction on heavier nuclei at lower energies. Perhaps the tails of the wave functions are poorly described by the theory and the reaction mechanism is oversensitive to them. Such sensitivity might result from the overlap of other form factors with the unbound He wave function which extends to infinity. Similar problems were revealed by the 14-MeV $(\alpha, 2\alpha)$ knockout measurements [15] which gave spectroscopic factors 2 orders of magnitude larger than predictions. Another possible explanation is that the standard approximations of the DWBA (e.g., neglecting $V_{3\alpha}$-$U_{\alpha\alpha}$) are tolerable for reactions on heavier nuclei but not on ^{4}He.

Further systematic intermediate-energy studies of unbound transfer reactions on light-to-intermediate targets could usefully employ heavy-ion beams and reverse kinematics. For example, the ^{12}C(^{4}He,^{5}He)^{11}B measurement [2] could be redone with a ^{12}C beam; the uncertainty of the coincidence detection efficiency for ^{5}He would be avoided by detecting ^{11}B recoils. Thus, (^{4}He,^{5}He) measurements on targets from ^{4}He to about ^{20}Ne might resolve the small-angle normalization problem revealed by the present measurement.

ACKNOWLEDGMENTS

We thank Professor C. M. Vincent and Professor J. R. Comfort for helpful correspondence and advice. We also thank the staff of the Research Center for Nuclear Physics for their excellent support during the experiment, which was performed at the RCNP under Program No. 31A16. The work was financially supported by grants from the National Science Foundation (PHY-8900070 and PHY-9122067), the Department of Energy (DE-FG02-87ER-40335), and the Oberlin College Research and Development Committee.

[1] N. Austern, *Direct Nuclear Reaction Theories* (Wiley, New York, 1970).
[2] A. Saha, R. Kamermans, J. van Driel, and H. P. Morsch, Phys. Lett. **79B**, 363 (1978).
[3] G. Baur and D. Trautmann, Phys. Rep. C **25**, 293 (1976).
[4] C. M. Vincent and H. T. Fortune, Phys. Rev. C **2**, 782 (1970).
[5] P. D. Kunz, A. Saha, and H. T. Fortune, Phys. Rev. Lett.

43, 341 (1979).
[6] F. Ajzenberg-Selove, Nucl. Phys. **A490**, 1 (1988).
[7] P. Darriulat, G. Igo, H. G. Pugh, and H. D. Holmgren, Phys. Rev. **137**, B315 (1965).
[8] E. A. Silverstein, Nucl. Instrum. Methods **4**, 53 (1959).
[9] R. E. Warner, A. M. van den Berg, K. M. Berland, J. D. Hinnefeld, Z. Zhang, Y. T. Zhu, X. Q. Hu, and S. Li, Phys. Rev. C **40**, 2473 (1989).
[10] P. D. Kunz, computer code DWUCK4 (unpublished).
[11] J. R. Shepard, E. Rost, and G. R. Smith, Phys. Lett. **89B**, 13 (1979).
[12] A. Nadasen, P. G. Roos, B. G. Glagola, G. J. Matthews, V. E. Viola, H. G. Pugh, and P. Frisbee, Phys. Rev. C **18**, 2792 (1978).
[13] B. Hoop and H. H. Barschall, Nucl. Phys. **83**, 65 (1966).
[14] J. R. Shepard, W. R. Zimmerman, and J. J. Kraushaar, Nucl. Phys. **A275**, 189 (1975).
[15] C. W. Wang, N. S. Chang, P. G. Roos, A. Nadasen, and T. A. Carey, Phys. Rev. C **21**, 1705 (1980).